Supplementary Material

A novel membrane anchor for FtsZ is linked to cell wall hydrolysis in *Caulobacter crescentus*

Elizabeth L. Meier[a], Shiva Razavi[b], Takanari Inoue[b,c] and Erin D. Goley[a,I]

[a]Department of Biological Chemistry, Johns Hopkins University School of Medicine, 725 N. Wolfe Street, Baltimore, Maryland 21205, USA
[b]Department of Biomedical Engineering, Johns Hopkins University School of Medicine, 720 Rutland Avenue, Baltimore, Maryland 21205, USA
[c]Department of Cell Biology, Johns Hopkins University School of Medicine, 855N. Wolfe Street, Baltimore, Maryland 21205, USA
[I]Correspondence and requests for materials should be addressed to E.D.G.
Address: Department of Biological Chemistry, Johns Hopkins University School of Medicine, 725 N. Wolfe Street, 520 Wood Basic Science Building, Baltimore, Maryland 21205, USA
Phone: 410-502-4931
Email: egoley1@jhmi.edu

Running title: Novel FtsZ membrane anchor linked to cell wall hydrolysis

Key words: FtsZ, FzlC, membrane, cell division, Caulobacter

Table S1. Growth rate and cell length of strains in Figs. 5 and 6

Strain	**Description (24 h o/e)**	**Doubling time ± SEM (hr)***	**Mean cell length ± SEM (μm)†**	**N**
EG890	Empty vector	1.94 ± 0.01	2.42 ± 0.02	800
EG891	*fzlC* o/e vector	2.07 ± 0.01	2.98 ± 0.04	800
EG1405	Empty vector; *xylX::*P_{xyl}*-ftsZ-yfp*	ND	2.95 ± 0.04	490
EG1406	*fzlC* o/e vector; *xylX::*P_{xyl}*-ftsZ-yfp*	ND	3.79 ± 0.05	578

* EG890 vs EG891 = $p < 0.001$ unpaired t test, two-tailed

† EG890 vs EG891, EG1405 vs EG1406 = $p < 0.001$ unpaired t test, two-tailed; N refers to sample size for cell length analysis.

Table S2. Growth rate and cell length of strains in Fig. S4

Strain	**Description**	**Doubling time ± SEM (hr)***	**Mean cell length ± SEM (μm)†**	**N**
EG864	WT	1.85 ± 0.004	2.46 ± 0.03	614
EG653	*fzlC::mChy-fzlC*	3.37 ± 0.2	4.03 ± 0.12	503
EG859	*fzlC::fzlC-mChy*	ND	2.73 ± 0.03	692
EG1445	*fzlC::yfp-fzlC*	1.95 ± 0.01	2.58 ± 0.03	551
EG444	*xylX::* P_{xyl}*-ftsZ-yfp*	ND	3.10 ± 0.04	383
EG1404	*fzlC::mChy-fzlC*; *xylX::* P_{xyl}*-ftsZ-yfp*	ND	4.78 ± 0.14	305

* EG864 vs EG653, EG1445 vs EG653 = $p < 0.001$; EG864 vs EG1445 = not significant (ns) ANOVA Tukey's Multiple Comparison Test

† EG864 vs EG653, EG859 vs EG653, EG1445 vs EG653 = $p < 0.001$; EG864 vs EG859 = $p < 0.01$; EG864 vs EG1445, EG859 vs EG1445 = ns ANOVA Tukey's Multiple Comparison Test; EG444 vs EG1404 = $p < 0.001$ unpaired t test, two-tailed; N refers to sample size for cell length analysis.

Table S3. Growth rate and cell length of strains in Fig. 7

Strain	Description	Doubling time ± SEM (hr)*	Mean cell length ± SEM (μm)†	N
Fig. 7A				
EG864	WT	2.14 ± 0.06	2.66 ± 0.04	700
EG289	*ΔfzlC*	2.08 ± 0.05	2.57 ± 0.03	700
Fig. 7B				
EG289	*ΔfzlC*	1.59 ± 0.01	3.03 ± 0.03	645
EG590	*ΔdipM*	2.93 ± 0.02	7.29 ± 0.36	347
EG1242	*ΔdipM ΔfzlC*	4.51 ± 0.17	9.25 ± 0.39	300
Fig. 7C				
EG864	WT	1.65 ± 0.004	2.52 ± 0.03	632
EG1133	*ΔftsE*	1.88 ± 0.005	3.51 ± 0.10	655
EG1162	*ΔftsE ΔfzlC*	2.60 ± 0.007	4.20 ± 0.13	585
Fig. 7D				
EG289	*ΔfzlC*	1.54 ± 0.05	2.34 ± 0.02	600
EG1756	*ΔamiC*	1.59 ± 0.01	2.32 ± 0.02	600
EG1771	*ΔamiC ΔfzlC*	1.53 ± 0.03	2.48 ± 0.03	600

* Fig. 7A: EG864 vs EG289 = ns; Fig. 7B: EG289 vs EG590, EG289 vs EG1242, EG590 vs EG1242 = $p < 0.001$; Fig. 7C: EG864 vs EG1133, EG864 vs EG1162, EG1133 vs EG1162 = $p < 0.001$; Fig. 7D: EG289 vs EG1756, EG289 vs EG1771, EG1756 vs EG1771 = ns ANOVA Tukey's Multiple Comparison Test

† Fig. 7A: EG864 vs EG289 = ns Mann Whitney test; 7B: EG289 vs EG590, EG289 vs EG1242, and EG590 vs EG1242 = $p < 0.001$; Fig. 7C = EG864 vs EG1133, EG864 vs EG1162, and EG1133 vs EG1162 = $p < 0.001$; Fig. 7D = EG289 vs EG1756 = ns, EG289 vs EG1771 and EG1756 vs EG1771 = $p < 0.001$ ANOVA Tukey's Multiple Comparison Test; N refers to sample size for cell length analysis.

Table S4. Growth rate and cell length of strains in Fig. S5

Strain	Description	Doubling time ± SEM (hr) *	Mean cell length ± SEM (µm) †	N
Fig. S5B				
EG289	*ΔfzlC*	1.59 ± 0.01	3.02 ± 0.04	600
EG1080	*ΔzapA*	1.82 ± 0.01	2.79 ± 0.04	600
EG1232	*ΔzapA ΔfzlC*	1.74 ± 0.01	3.20 ± 0.05	600
Fig. S5C				
EG289	*ΔfzlC*	1.55 ± 0.06	2.62 ± 0.03	600
EG1289	*ΔkidO*	1.66 ± 0.04	2.99 ± 0.06	600
EG1298	*ΔkidO ΔfzlC*	1.56 ± 0.07	3.08 ± 0.06	600
Fig. S5D				
EG289	*ΔfzlC*	1.78 ± 0.05	2.85 ± 0.03	600
EG1290	*ΔtipN*	2.26 ± 0.02	4.37 ± 0.13	600
EG1299	*ΔtipN ΔfzlC*	2.26 ± 0.04	4.19 ± 0.11	600
Fig. S5E				
EG289	*ΔfzlC*	1.78 ± 0.05	2.85 ± 0.03	600
EG1305	*ΔftsB*	2.03 ± 0.01	3.02 ± 0.04	600
EG1307	*ΔftsB ΔfzlC*	2.14 ± 0.02	2.83 ± 0.03	600
Fig. S5F				
EG289	*ΔfzlC*	1.55 ± 0.005	2.32 ± 0.02	600
EG1189	*Δpbp1a ΔpbpY ΔpbpC ΔpbpZ ΔmtgA*	1.76 ± 0.02	2.49 ± 0.02	600
EG1509	*Δpbp1a ΔpbpY ΔpbpC ΔpbpZ ΔmtgA ΔfzlC*	1.89 ± 0.03	2.25 ± 0.02	600

* Fig. S5B: EG289 vs 1080, EG289 vs EG1232 = p <0.001, EG1080 vs EG1232 = p <0.01; Fig. S5C: all strain combinations were ns; Fig. S5D: EG289 vs EG1290, EG289 vs EG1299 = p <0.001, EG1290 vs EG1299 = ns; Fig. S5E: EG289 vs 1305 = p <0.01, EG289 vs EG1307 = p <0.001, EG1305 vs EG1307 = ns; Fig. S5F: EG289 vs EG1189, EG289 vs EG1509 = p <0.001, EG1189 vs EG1509 = p <0.01 ANOVA Tukey's Multiple Comparison Test

† Fig. S5B: EG289 vs EG1080, EG1080 vs EG1232 = $p < 0.001$, EG289 vs EG1242 = ns;
Fig. S5C: EG289 vs EG1289, EG289 vs EG1298 = $p < 0.001$, EG1289 vs EG1298 = ns;
Fig. S5D: EG289 vs EG1290, EG289 vs EG1299 = $p < 0.001$, EG1290 vs EG1299 = ns;
Fig. S5E: EG289 vs EG1305, EG1305 vs EG1307 = $p < 0.01$, EG289 vs EG1307 = ns;
Fig. S5F: EG289 vs EG1189, EG1189 vs EG1509 = $p < 0.001$, EG289 vs EG1509 = ns,
ANOVA Tukey's Multiple Comparison Test; N refers to sample size for cell length analysis.

Table S5. Growth rate and cell length of strains in Fig. 9

Strain	**Description (24 h o/e)**	**Doubling time ± SEM (hr)***	**Mean cell length ± SEM (μm)†**	**N**
EG1357	Empty vector; *ΔftsE*	2.91 ± 0.04	3.55 ± 0.08	650
EG1346	*fzlC* o/e vector; *ΔftsE*	2.84 ± 0.04	2.94 ± 0.04	650
EG1380	Empty vector; *ΔftsE xylX::* P_{xyl}*-ftsZ-yfp*	ND	5.17 ± 0.12	528
EG1379	*fzlC* o/e vector; *ΔftsE xylX::* P_{xyl}*-ftsZ-yfp*	ND	4.02 ± 0.06	525

* EG1357 vs EG1346 = ns unpaired t test, two-tailed

† EG1357 vs EG1346, EG1380 vs EG1379 = *p* value < 0.001 unpaired t test, two-tailed; N refers to sample size for cell length analysis.

Supplementary Figures

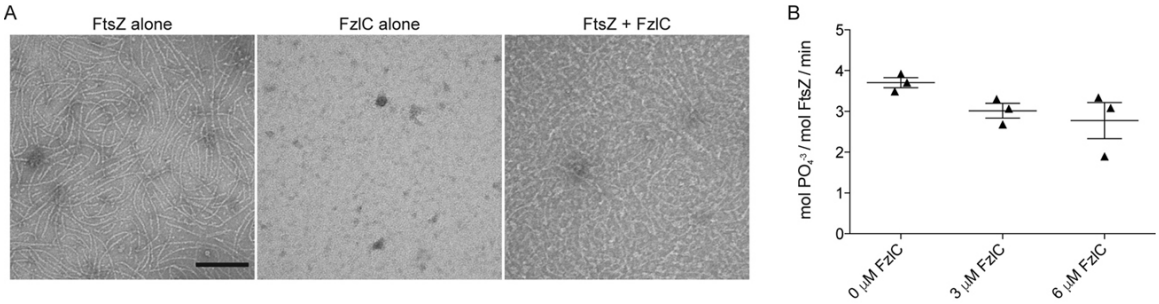

Figure S1. FzlC does not affect FtsZ polymer structure or GTPase activity. (A) Electron micrographs of purified FtsZ, YFP-FzlC, or FtsZ and YFP-FzlC. All reactions contained 4 μM protein, 2 mM GTP (in reactions containing FtsZ), and 2.5 mM $MgCl_2$. Scale bar = 100 nm (B) GTPase rate measured as the amount of inorganic phosphate released over time by 3 μM FtsZ as a function of increasing FzlC concentration. Error bars represent mean GTPase rate ± standard error of the mean (SEM) from three experimental replicates taken from two experiments performed on separate days.

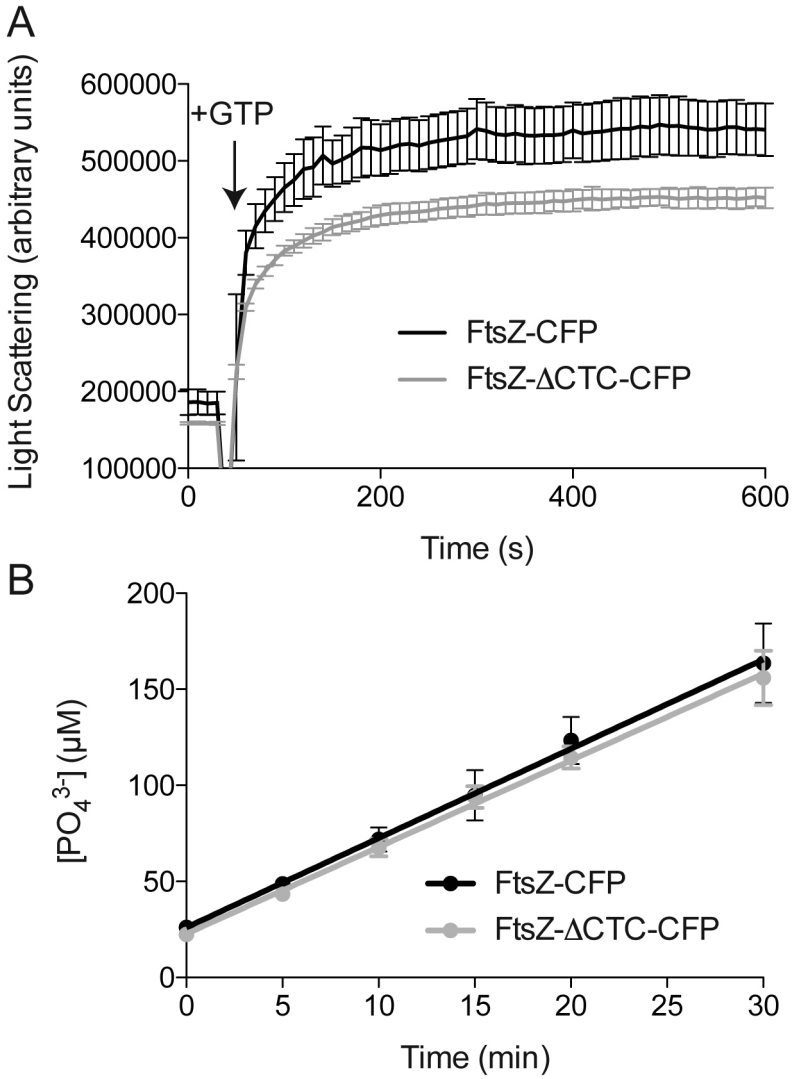

Figure S2. FtsZ-CFP and FtsZΔCTC-CFP display similar polymerization activities. (A) Right angle light scattering over time for solutions of 2 μM FtsZ-CFP or FtsZΔCTC-CFP. GTP was added to 2 mM to induce polymerization when indicated with the arrow. Mean ± SEM for three replicates is shown. (B) Inorganic phosphate concentration over time for solutions of 2 μM FtsZ or FtsZΔCTC. Mean ± SEM is shown for three replicates. Lines are linear regressions fit to the data.

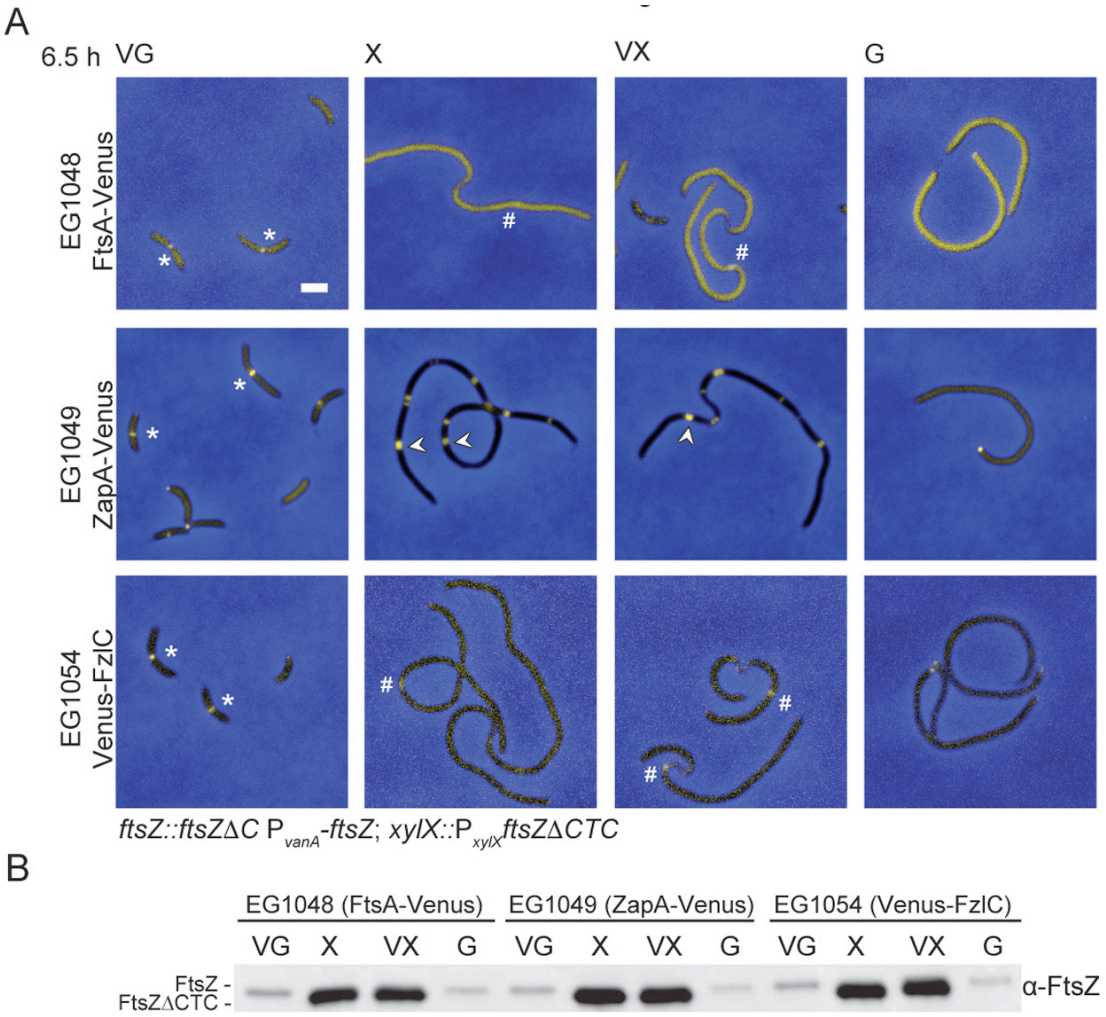

Figure S3. FzlC requires the CTC to localize to Z-rings *in vivo*. (A) Merged fluorescent (yellow) and phase contrast (blue) micrographs of cells with vanillate inducible *ftsZ* and xylose inducible *ftsZΔCTC* expressing either *ftsA-venus* (EG1048), *zapA-venus* (EG1049), or *venus-fzlC* (EG1054) on a low copy replicating plasmid under the control of its own promoter grown with the indicated inducers for 6.5 h. The white asterisks denote localization to focused Z-rings, the white arrowheads denote localization to wider Z-rings, and # denotes weak localization. Scale bar = 2 μm. (B) Immunoblot of FtsZ or FtsZΔCTC levels in the strains from (A). FtsZΔCTC was present at much higher levels than FtsZ, presumably because it lacks the C-terminal degradation sequence recognized by the ClpXP protease. V = vanillate; X = xylose; G = glucose.

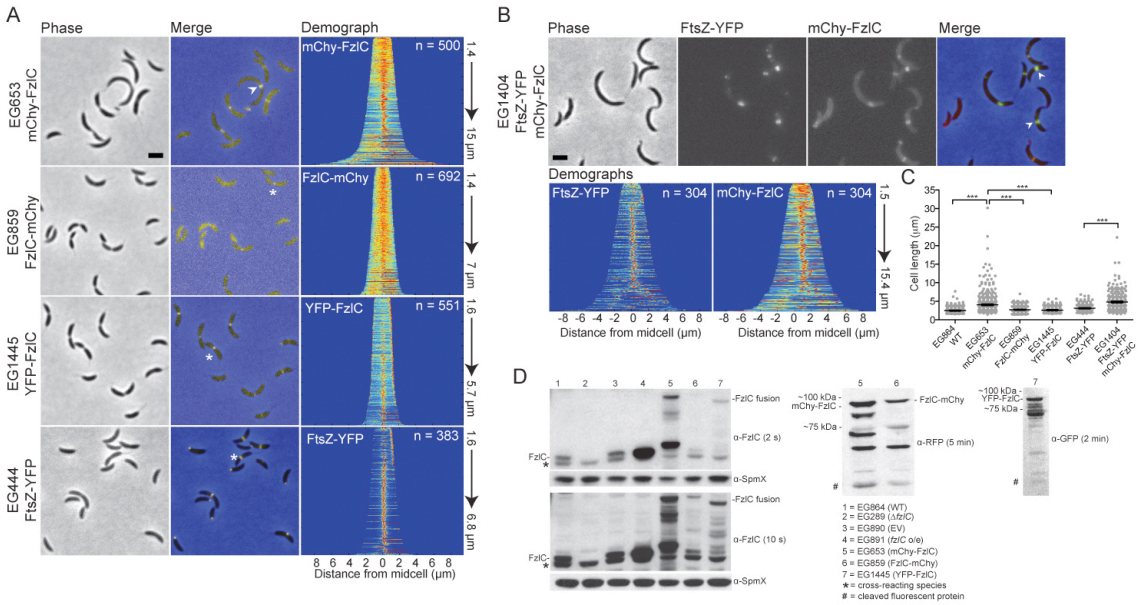

Figure S4. Differentially tagging FzlC affects FzlC localization, cellular morphology and FzlC protein levels. (A) Phase contrast and merged micrographs (phase contrast in blue and fluorescence in yellow) of cells with *mChy-fzlC* (EG653), *fzlC-mChy* (EG859), or *yfp-fzlC* (EG1445) at the native *fzlC* locus as the only copy of *fzlC* or of xylose inducible *ftsZ-yfp* at the *xylX* locus in a WT background (EG444). Demographs (far right) represent normalized signal profiles of fluorescent fusions to FzlC or FtsZ in cells arranged by increasing cell length. White asterisks denote focused FzlC or Z-rings and the white arrowheads denote more diffuse FzlC or Z-rings. Scale bar = 2 μm. (B) Phase contrast, fluorescence, and merged micrographs (phase contrast in blue and fluorescence in red (FzlC) or green (FtsZ)) of cells with *mChy-fzlC* at the native *fzlC* locus as the only copy of *fzlC* and xylose-inducible *ftsZ-yfp* (EG1404). Demographs represent normalized signal profiles of fluorescent fusions to FzlC or FtsZ in cells arranged by increasing cell length. (C) Cell lengths of strains in (A) (see Table S2 for sample sizes). Error bars represent the mean cell length ± SEM, *** = $p < 0.001$, one-way ANOVA. (D) Immunoblots of cell lysates from strains from (A) and Fig. 5 probed for FzlC and, when appropriate, RFP (EG653 and EG859) or GFP (EG1445). SpmX was used as a loading control. Two different exposure times for the α-FzlC immunoblot (2 sec or 10 sec) are presented for better visualization of FzlC levels in the different strains.

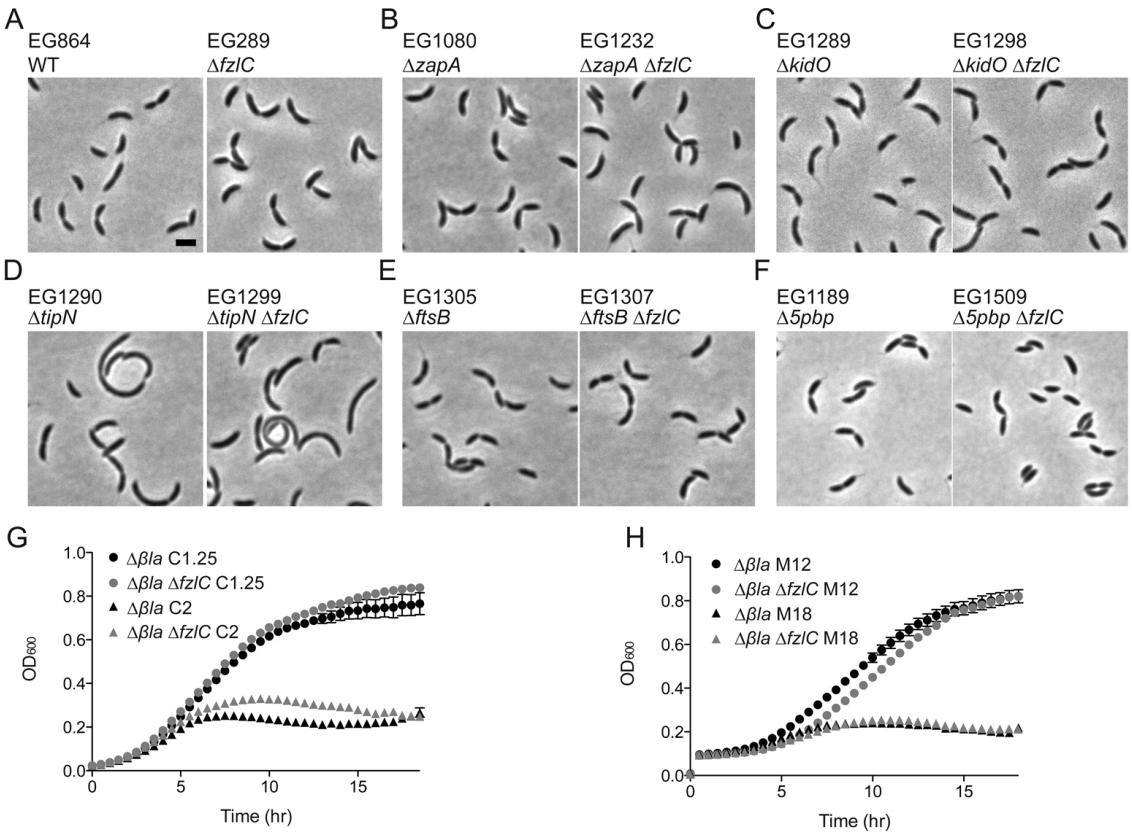

Figure S5. *fzlC* does not interact genetically with many non-essential division genes. (A-F) Phase contrast micrographs of cells with or without *fzlC* in WT and in non-essential gene mutant backgrounds. Scale bar = 2 μm. "*Δ5pbp*" = *Δpbp1a ΔpbpY ΔpbpC ΔpbpZ ΔmtgA* (G) Growth curves of *Δβla* (EG1121, lacking the primary β-lactamase) and *Δβla ΔfzlC* (EG1504) cells treated with cephalexin at sublethal (1.25 μg/mL (C1.25)) or lethal (2 μg/mL (C2)) concentrations. (H) Growth curves of EG1121 and EG1504 treated with mecillinam at sublethal (12 μg/mL (M12)) or lethal (18 μg/mL (M18)) concentrations.

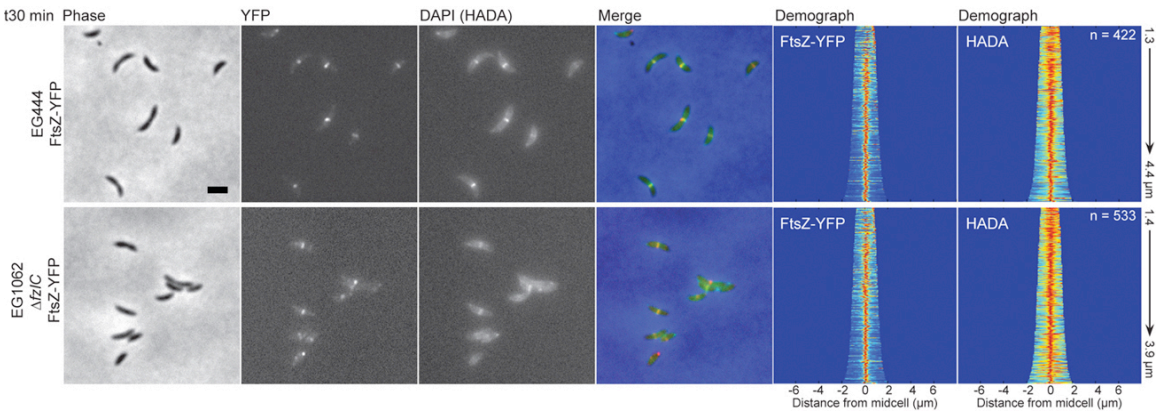

Figure S6. Z-rings still assemble and direct new cell wall synthesis in *ΔfzlC* cells. Phase contrast, fluorescent and merged micrographs of cells with xylose-inducible *ftsZ-yfp* at the *xylX* locus in a WT (EG444) or *ΔfzlC* (EG1062) background that were synchronized, pulse-labelled with HADA for 5 min at 30 min post-synchrony, and imaged. In the merged image, FtsZ-YFP is in red and HADA is in green. Demographs represent signal profiles of FtsZ-YFP or HADA in cells arranged by increasing cell length. Scale bar = 2 µm.

Supplementary References

Bendezú F.O., Hale C.A., Bernhardt T.G., de Boer P.A. (2009) RodZ (YfgA) is required for proper assembly of the MreB actin cytoskeleton and cell shape in *E. coli*. *EMBO J* **28**:193-204.

Evinger M., Agabian N. (1977) Envelope-associated nucleoid from *Caulobacter crescentus* stalked and swarmer cells. *J Bacteriol* **132**:294-301.

Goley E.D., Comolli L.R., Fero K.E., Downing K.H., Shapiro L. (2010a) DipM links peptidoglycan remodelling to outer membrane organization in *Caulobacter*. *Mol Microbiol* **77**:56-73.

Goley E.D., Dye N.A., Werner J.N., Gitai Z., Shapiro L. (2010b) Imaging-based identification of a critical regulator of FtsZ protofilament curvature in *Caulobacter*. *Mol Cell* **39**:975-87.

Goley E.D., Yeh Y.C., Hong S.H., Fero M.J., Abeliuk E., McAdams H.H., Shapiro L. (2011) Assembly of the *Caulobacter* cell division machine. *Mol Microbiol* **80**:1680-98.

Huitema E. Pritchard S., Matteson D., Radhakrishnan S.K., Viollier P.H. (2006) Bacterial birth scar proteins mark future flagellum assembly site. *Cell* **124**:1025-37.

Moll A., Schlimpert S., Briegel A., Jensen G.J., Thanbichler M. (2010) DipM, a new factor required for peptidoglycan remodeling during cell division in *Caulobacter crescentus*. *Mol Microbiol* **77**:90-107.

Radhakrishnan S.K., Pritchard S., Viollier P.H. (2010) Coupling prokaryotic cell fate and division control with a bifunctional and oscillating oxidoreductase homolog. *Dev Cell* **18**:90-101.

Schrader J.M. *et al*. (2014) The coding and noncoding architecture of the *Caulobacter crescentus* genome. *PLoS Genet* **10**:e1004463.

Stephens C., Mohr C., Boyd C., Maddock J., Gober J., Shapiro L. (1997) Identification of the fliI and fliJ components of the *Caulobacter* flagellar type III protein secretion system. *J Bacteriol* **179**:5355-65.

Sundararajan K., Miguel A., Desmarais S.M., Meier E.L., Casey Huang K., Goley E.D. (2015) The bacterial tubulin FtZ requires its intrinsically disordered linker to direct robust cell wall construction. *Nat Commun* **6**:7281.

Thanbichler M., Iniesta A.A., Shapiro L. (2007) A comprehensive set of plasmids for vanillate- and xylose-inducible gene expression in *Caulobacter crescentus*. *Nucleic Acids Res* **35**:3137.

Thanbichler M., Shapiro L. (2006) MipZ, a spatial regulator coordinating chromosome segregation with cell division in *Caulobacter*. *Cell* **126**:147-62.

Wang Y., Jones B.D., Brun Y.V. (2001) A set of *ftsZ* mutants blocked at different stages of cell division in *Caulobacter*. *Mol Microbiol* **40**:347-60.

Weiner M.P. *et al* (1994) Studier pET system vectors and hosts. *Strategies Mo Bio* **7**:41-43.

Yakhnina A.A., Gitai Z. (2013) Diverse functions for six glycosyltransferases in *Caulobacter crescentus* cell wall assembly. *J Bacteriol* **195**:4527-35.